Dynamics of erosion processes in the tropics: a dendrogeomorphological approach in an Ultisol of southeastern Brazil

Renata Cristina Bovi, Marcelo Pablo Chartier, Fidel Alejandro Roig, Mario Tomazello Filho, Virginia Dominguez Castillo, et al.

Plant and Soil
An International Journal on Plant-Soil Relationships

ISSN 0032-079X

Plant Soil
DOI 10.1007/s11104-019-04227-2

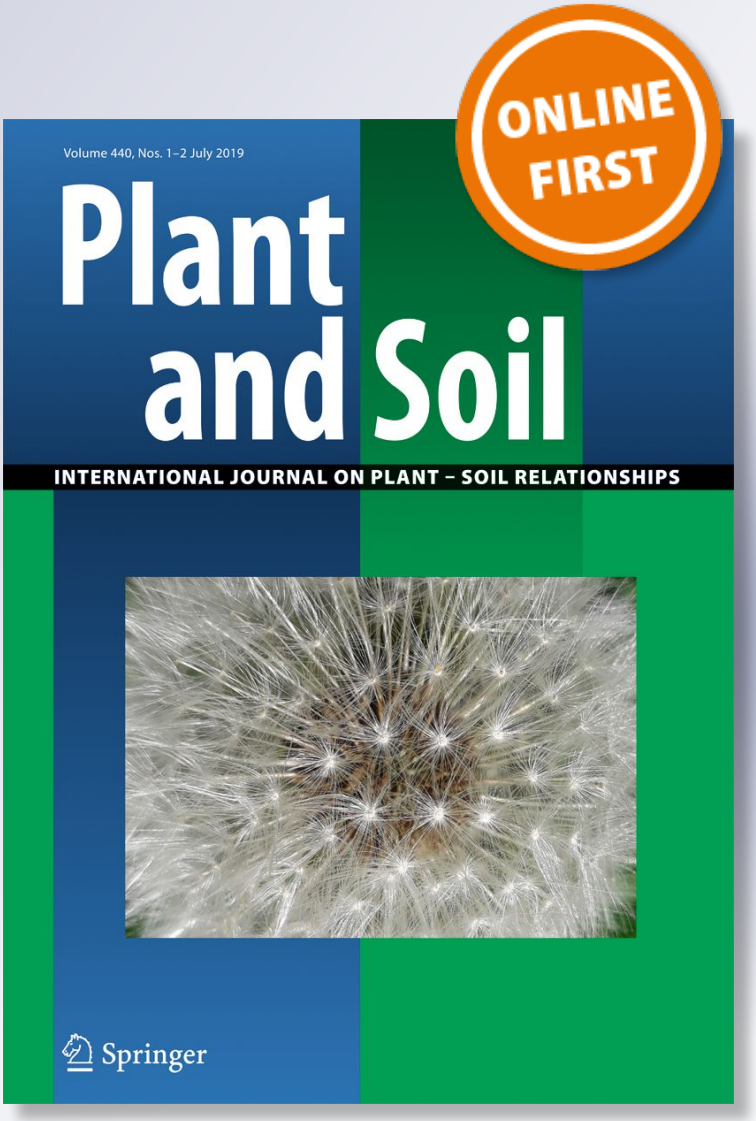

Springer

Plant Soil
https://doi.org/10.1007/s11104-019-04227-2

REGULAR ARTICLE

Dynamics of erosion processes in the tropics: a dendrogeomorphological approach in an Ultisol of southeastern Brazil

Renata Cristina Bovi · Marcelo Pablo Chartier · Fidel Alejandro Roig · Mario Tomazello Filho · Virginia Dominguez Castillo · Miguel Cooper

Received: 2 April 2019 / Accepted: 16 July 2019

Abstract

Background and aims Soil erosion is one of the degradation processes that historically has caused great impacts on agricultural activities and the environment. It is responsible for soil loss, reduced productivity and various environmental impacts. Given the importance of research related to understanding the soil erosion process, the dendrogeomorphology technique has a significant role in qualifying and quantifying this degradation process. It is a technique that uses the structure of the root and stem wood of trees affected by erosion processes to date these events and measure the rate of soil loss. The objective of this study was to understand the dynamics of the erosion process through the dendrogeomorphological approach.

Methods The changes in growth pattern of exposed roots of *Esenbeckia leiocarpa* trees (guarantã) were studied, such as growth ring width, eccentricity, vessel frequency and scars.

Results The results obtained demonstrated the potential of the species for dendrogeomorphological studies, since the changes in growth patterns after

Responsible Editor: Amandine Erktan.

Electronic supplementary material The online version of this article (https://doi.org/10.1007/s11104-019-04227-2) contains supplementary material, which is available to authorized users.

R. C. Bovi · M. T. Filho · V. D. Castillo · M. Cooper (✉)
Luiz de Queiroz School of Agriculture, University of São Paulo (USP), Av. Pádua Dias 11, Piracicaba, (SP) CEP 13418-900, Brazil
e-mail: mcooper@usp.br

R. C. Bovi
e-mail: bovirc@gmail.com

M. T. Filho
e-mail: mtomazel@usp.br

V. D. Castillo
e-mail: v.domcas@gmail.com

M. P. Chartier
Instituto de Investigaciones Biológicas y Tecnológicas, Centro de Ecología y Recursos Naturales Renovables (CONICET – Universidad Nacional de Córdoba), Av. Vélez Sarsfield 1611, X5016GCA Córdoba, Argentina
e-mail: mpchartier@gmail.com

F. A. Roig
Instituto Argentino de Nivología, Glaciología y Ciencias Ambientales- IANIGLA -CONICET, Laboratorio de Dendrocronología e Historia Ambiental, Mendoza, Argentina
e-mail: froig@mendoza-conicet.gob.ar

F. A. Roig
Facultad de Ciencias Agrarias, Universidad Nacional de Cuyo, Mendoza, Argentina

F. A. Roig
Facultad de Ciencias, Hémera Centro de Observación de la Tierra, Universidad Mayor, Santiago de Chile, Chile

Published online: 03 August 2019

exposure allowed to date the first year of root exposition.

Conclusions The dendrogeomorphology technique proved to be effective in understanding the process dynamics of complex systems, such as the opening of permanent and ephemeral gullies. In addition, it is effective in inferring soil loss rates.

Keywords Exposed root · Dating · Dendrochronology · Piping · Gully

Introduction

Soil erosion is a key driver of land degradation process that historically has caused significant impacts in many environments worldwide (Lal 2001; Poesen 2018). Although erosive processes have existed throughout the history of agriculture, this has intensified during the twenty-first century (Lal 2001; Pimentel et al. 1995) with forecasts of greater severity depending on land degradation and climate change, particularly in tropical and subtropical lands (Lal 2001).

Because no resource or environmental management problem can be rationally addressed until the real dimensions of time and space are known (Trimble and Crosson 2000), new research to improve our understanding of soil degradation processes is increasingly important. Erosion and deposition processes are at the heart of the explanation of the geomorphological evolution of relief but essential information about the dynamics of landscape change have been difficult to obtain (Lawler 2005).

The method of dendrogeomorphology is based on the determination of the influence of the geomorphological processes that affects the dynamics of tree growth. These are evidenced by changes in anatomical indicators such as the annual growth patterns and anatomy of the growth rings, the concentric regularity of the stem transversal section, growth rates and anatomy of the wood (e.g., number of cells per ring, cell lumen diameter of the earlywood cells, percentage of latewood) (Hitz et al. 2008).

A characterization of the anatomical changes in a certain growth ring may indicate the temporary onset of a root exposure. From this information, the rate of soil loss can be inferred (up to the date of root harvesting), as a result of crossing data from the measure of soil surface retraction against a datable surface, that means, the exposed root (Lawler 2005). According to Gärtner et al. (2001), the anatomical changes in the growth rings are related to the effects of root exposure to the atmosphere, such as variations in temperature, reduction of soil cover pressure or incidence of light, but also to the mechanical stress that occurs in the root when it loses the edaphic cover continuously and progressively. Exposed roots and tree trunks have been used in dendrogeomorphology research since the 1960s to determine erosion rates exclusively in temperate climates (Bodoque et al. 2015), posing a great challenge to the use of this technique in tropical tree species (Stoffel et al. 2013). The advantage of dendrogeomorphology, when compared to conventional techniques for soil erosion measures, is that erosion rates can be quantified with annual resolution at average rates and also for single events (Ballesteros-Cánovas et al. 2013).

In this study, we describe the anatomical responses and changes in the pattern of root growth subjected to exposure due to erosive processes in a native hardwood tropical tree species growing on Hapludult-type soils in southeastern Brazil. We identified the beginning of erosion by application of dating methods of the anatomical alterations identified in the exposed roots of this tree, aiming to reconstruct the dynamics of the erosive process and to infer soil loss rates. The results of the present study can be extrapolated to other regions with the same type of soil, being relevant to warn about the dangers of soil loss in agricultural areas that sustain large economies in the Neotropics.

Material and methods

Study area

The study area is part of the Experimental Station of Tupi, located in the county of Piracicaba, state of São Paulo, Brazil (Online Resource 1). In the first half of the twentieth century this area was transformed into crops (cotton, coffee, sugar cane) after deforestation and later reforested with exotic and native tree species during the 1960s.

The climate of the region is tropical humid, classified as Cwa according to Köppen (Köppen classification) (Alvares et al. 2013a), with a wet summer and dry winter that determines the climatic seasonality of the region. The mean total precipitation is 1275 mm year^{-1}, with the rainiest period between December and February (mean rainfall of 610 mm) and the driest period between June and August (mean rainfall of 101 mm).

The annual average temperature is 21.4 °C, with an annual maximum mean of 28.2 °C and an annual minimum mean of 14.8 °C (Alvares et al. 2013b).

The study site is located in the Paulista Peripheral Depression with moderate undulating landscapes with local slopes that vary from 12 to 57% and altitudes varying from 505 to 565 m above sea level (Vidal-Torrado and Lepsch 1999). In the field, active soil erosion is mainly evidenced, from initial processes of degradation – sheet erosion - to the most advanced, such as permanent gullies and subsurface erosions (piping). The dominant soil was classified as Typic Hapludult. Ultisols and Oxisols are the most expressive soils of Brazil and occupy, respectively, 24% and 39% of the total area of the country (IBGE 2007; Santos et al. 2011). Classification of soils was according to the Soil Survey Staff (1999). The parent material is composed of sandstones, belonging to the Itararé Group. The soils have an approximate depth of 1.7 m; the surface horizons are moderately well drained, sandy textured (clay content less than 100 g kg-1); the subsurface horizons are poorly drained, with a medium texture (clay content between 200 and 220 g kg-1).

Selection of tree species

For this study, the semi-deciduous species *Esenbeckia leiocarpa* (guarantã), a tree native from Brazil and belonging to the Rutaceae family, was selected. The selection of the tree species was based on the presence of distinct annual growth rings, already referenced in the literature.

The anatomical structure that defines the limit of the growth rings consists of a combination of marginal parenchyma, a thick-walled latewood fibers and changes in vessel diameter (Lisi et al. 2008). Changes in leaf biomass are linked to partial loss of leaves during the dry winter season (July and August) and development of new leaves at the beginning of the rainy season (Lisi et al. 2008). This phenological behavior is probably linked to the good demarcation of the growth rings.

Field sampling

Root samples were collected in July 2014. Exposed roots were sampled from 22 trees that were affected by soil erosion and buried roots were collected from 10 trees without evidence of soil erosion. In both situations, one to two roots were collected per tree and one to two cross sections per root. Before the sample collection of each exposed root, the erosive process was classified, as: sheet erosion, ephemeral gullies, permanent gullies and subsurface erosion (piping). Permanent were differentiated from ephemeral gullies when surpassed 50 cm in depth (Poesen et al. 2003; Woodward 1999). The roots were collected with the use of a chainsaw, obtaining transverse sections of approximately 2″ thick. Before cutting, measurements of the exposed root height up to the current surface of the soil were performed every 10 cm. The roots were collected at a minimum distance of 0.5 to 1.5 m from the stem, since at smaller distances, root morphology may be influenced by stem growth (Corona et al. 2011; Gärtner 2007; Hitz et al. 2008). During the root collection, the upper part of the root and the direction of impact of the water flow were identified in the cross-sections. Figure 1 shows the digital elevation model with the erosion process localization and the spatial distribution of the arboreal individuals.

Dendrochronological analysis

The root cross sections were allowed to air-dry for ~30 days and then sanded sequentially with 60 to 1200 grit sanding belts. Identification and demarcation of the growth rings were performed in a binocular microscope; for each polished cross-section, three rays were demarcated. Then, high-resolution images (1200 dpi) of the cross-sections were obtained, and the growth rings were measured in millimeters using Image-Pro Plus software (version 4.5.0.29), with an accuracy of 0.01 mm.

For the control and correct dating of the growth rings and the identification of possible false, discontinuous or absent growth rings, the statistical cross-dating procedure was used in the COFECHA program (Holmes 1983). The annual series of growth rings were filtered using the cubic spline function, with the segments examined being 20 years with a 10-year overlap. For the identification of false growth rings, the continuity of each ring was monitored in the cross-section of each sample. As only live roots were collected, the last growth ring corresponded to the year in which the sampling was done (Hitz et al. 2008). Some rays had absent or thin growth rings due to the high eccentricity and deformation of the exposed roots, which made difficult to measure and cross-date rings. To solve the problem, a value of 0.01 mm was assigned to the missing rings (Howell and Mathiasen 2004). We synchronized measurements of growth rings from 40 exposed roots of 22 individuals and nine buried

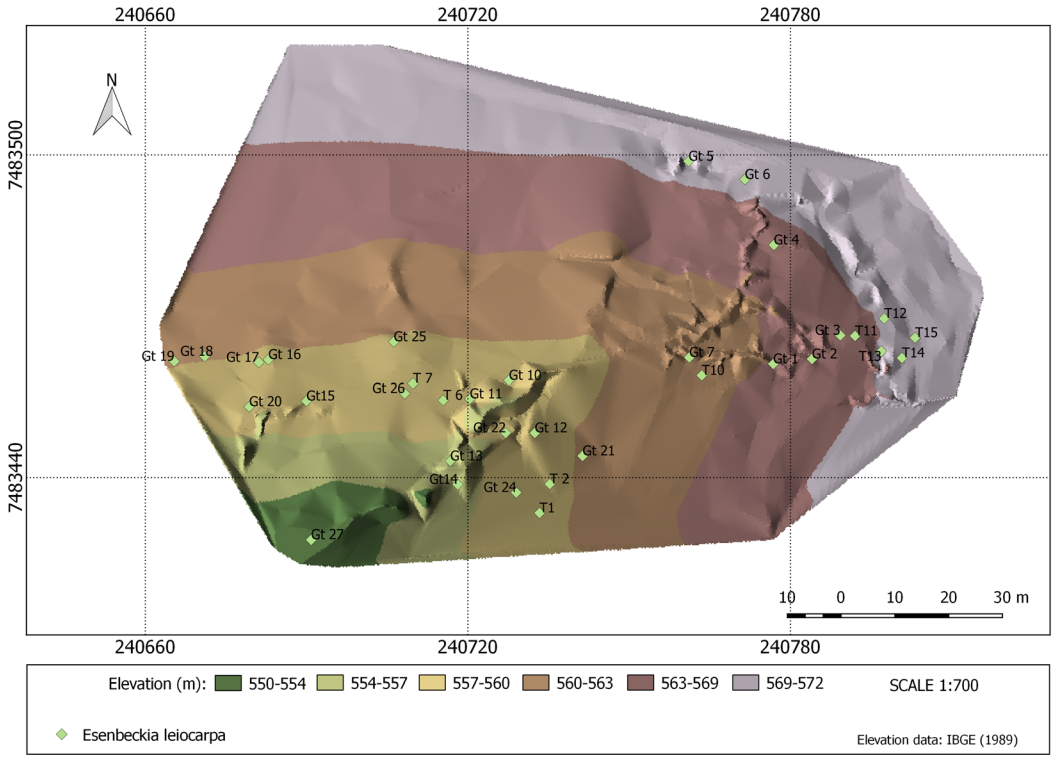

Fig. 1 Digital elevation model of the study site (red area in Online Resource 1) and localization of the trees: affected by soil erosion (prefix Gt) and control (T prefix)

roots from 8 trees. For four exposed roots, due to the high eccentricity or deformation of the growth rings, it was not possible to perform cross-dating with other samples; these samples were taken from the statistical analysis, and only visual cross-dating was performed.

Geomorphological events and the first year of root exposure dating

The following tree ring indicators were used to detect the first year of exposure linked to the soil erosion process: 1) growth ring width, 2) growth ring eccentricity and 3) vessel frequency (vessels/mm^2); as an auxiliary indicator, the presence of root scars in wood was used. Abrupt changes in these parameters were used to date the first year of root exposition. The methodologies used for the determination of the tree ring indicators are detailed below:

Growth ring width: corresponding to the mean annual growth ring measurements of three radii from each cross-section of the exposed roots.

Eccentricity: derived from the calculation of the growth ring eccentricity index performed by adapting the eccentricity index suggested by Šilhán and Stoffel (2015) and developed by Braam et al. (1987) for dating landslide and mass movements. Initially, the index (values between 0 and 1) is calculated using the following equation:

$$E = \left(\frac{a - c}{a + c} \right) \quad (1)$$

where a is the width of the growth ring of the eccentric radius and c is the width corresponding to the growth ring of a perpendicular position (90 °) to that radius. However, for the analyzed species in this study, there is not only one direction for the growth eccentricity. To solve this problem, the eccentricity index was calculated for the largest and smallest width of the same growth ring, among the three radii measured in each sample.

Vessel frequency: for the exposed roots, after verifying an abrupt change in the eccentricity index of the growth rings, the number of vessels (vessels mm^{-2}) was counted for the three years before and three years after the year showing any abrupt change in eccentricity. In the case of buried roots (control), the count was performed for all growth rings, except for those very narrow rings because of the difficulty in counting the vessels. This count was performed using high-resolution images (2400 dpi) of the

samples. For counting the number of vessels, a band of 1 mm in length was demarcated at the beginning and the end of the growth ring. Within this area, the number of vessels was counted. After this count, the area corresponding to this rectangle was determined, and the number of vessels was transformed into an area of 1 mm^2, as suggested by IAWA (1989).

Scars: the scars in the cross sections of the exposed roots were dated. For each scar, the approximated angle of its position was determined, respecting the same position found in the field.

All the anatomical parameters selected were analyzed together for the determination of the first year of exposure. The first growth ring with all the anatomical changes was determined as the growth ring relative to the initial exposure (called zero ring).

For the data analysis, a nonparametric ANOVA was used to determine the statistical differences for the growth ring width, eccentricity, and frequency of vessels per mm^2 for the three years before and three years after the year determined as the year of exposure of the root. A preliminary Shapiro-Wilk test was used to determine the normality of the data. As the data obtained had a non-normal distribution, the non-parametric Kruskal Wallis test was used. Statistical analyzes were performed with the Infostat program (version 2016). The level of significance was set at $p < 0.05$.

Determination of erosion rate

Two references were used to calculate the rate of soil loss:

1) Gärtner (2007) - eq. 2: in this equation, the average rate of soil loss was obtained by the value of the eroded soil layer (between the root and the current soil surface) and the exposure time determined in each exposed root. In this work, this calculation will be called vertical erosion rate.

$$\left[v_{er}/\text{cm year}^{-1}\right] = \left[h_{er}/\text{cm}\right]/\left[n_{ex}/\text{year}\right] \quad (2)$$

where:

v_{er} average vertical erosion rate (cm / year);
h_{er} height of the root exposed to the current soil surface;
n_{ex} difference in the number of growth rings (date of the first year of the root exposure to the year of sampling).

2) Malik (2008) - eq. 3: calculated considering the distance between two adjacent roots, arranged in parallel form in an erosive feature, divided by the exposure time of these neighboring roots. It was used exclusively for trees that had neighboring roots and parallel to each other. In this work, we call this equation horizontal erosion rate, which is representative of the backward erosion process of the gully head.

$$Her\ (cm/year) = \frac{(distance\ between\ roots)}{(difference\ in\ the\ exposure\ of\ these\ two\ roots)} \quad (3)$$

For the determination of the average vertical and horizontal soil erosion rates, we divided the study area into three sectors, according to the morphology of the main gully and the shape of the landscape (Online Resource 2). Changes in the gully morphology separate Sector I and Sector II. Sector I present a shallower and branched process and sector II a deeper and less branched gulling process. At the junction of Sector I and Sector II, there is a representative feature of the junction of two different linear erosive processes: an "erosion step" (brown circle of Online Resource 2). The presence of discontinuous erosive processes and not connected to the central gully characterize Sector III. For the calculation of the average soil loss, the different types of erosion processes were considered separately.

Meteorological data

The meteorological data for the analysis of the erosive rainfall events were acquired through automatic stations installed at the University of São Paulo, distant approximately 12 km from the study area and which data is available at http://www.leb.esalq.usp.br/posto/. For the analysis of the erosive rains, the period analyzed covers the years 1997 to 2013, due to the availability of the

data. The data of the acquired rainfall intensities were classified in intervals, namely: 25 to 50 mm/h, 50 to 75 mm/h and greater than 75 mm/h. For tropical and subtropical countries, rainfall is classified as erosive when they have intensities higher than 25 mm/h (Hudson 1965). From these data, the number of erosive events was counted, and correlated with the total precipitation, to understand the relation of erosive rains to the total precipitation.

Results

Dendrochronological dating of growth rings series

The root samples of exposed and buried roots analyzed showed growth rings anatomically demarcated and macroscopically visible. In exposed roots, the formation of discontinuous growth rings was observed, due to vascular cambium reactions or high eccentricity after exposure. In the same way, the presence of double or multiple rings was identified, being checked and corrected for the accurate dating by cross-dating with other samples (Ballesteros-Cánovas et al. 2013) through the COFECHA software.

For the exposed roots, the ages of the samples ranged from a minimum of 13 years to a maximum of 38 years, with a mean inter-correlation of 0.435 and a mean sensitivity of 0.530 (99% confidence). For the exposed roots, 84 growth ring series of 40 exposed roots from 22 trees were inter-correlated. For the buried root samples, the minimum age found was 20 years and a maximum of 40 years was recorded, with an average inter-correlation of 0.470 and mean sensitivity of 0.527 (99% confidence). A total of 22 growth ring series of 9 buried roots (control) from 8 trees were considered in the analysis.

Tree ring indicators for dating the first year of exposure

All the exposed root samples analyzed showed changes in the anatomical parameters compared to the buried root samples, namely: eccentricity, vessel frequency, appearance of scars and change in the width of growth rings (Figs. 2 and 3).

Figure 4a shows the growth ring width analysis of all the exposed roots, relating the years determined as before and after the exposure process and the year of exposure (year zero). A width increase in the first growth ring after exposure (year 1) is noted. In the following growth rings, a decrease in the width of the rings is observed.

All samples of exposed roots showed an increase in the eccentricity index in the most recent growth rings after the root exposure. The growth ring eccentricity index of the exposed roots samples presented an increase of 40.3% when compared to the average of the rings considered as year zero (year of exposure) and year 1 (first year after exposure). The eccentricity of the unexposed growth rings of the exposed roots (years −3, −2 and − 1) presented significant differences when compared to the growth rings that grew after exposure (years 1, 2 and 3). In other words, after the occurrence of soil erosion and consequent root exposure, there was an evident and significant increase in the eccentricity of the growth rings (Fig. 4b).

Roots lost concentricity of the rings when exposed, passing from a concentric growth to eccentric growth of the rings (Fig. 3). Comparing the eccentricity indexes of the growth rings before and after the erosive process with the eccentricity indexes of the growth rings of control roots samples, a statistically significant difference was observed between the three groups analyzed (Fig. 4c). The growth rings of the control samples showed significant differences in the eccentricity indexes when compared to the unexposed growth rings of the exposed roots. Figure 5 shows that *Esenbeckia leiocarpa* presents an intrinsic and natural eccentricity index of the growth rings, with values reaching a maximum of 0.50. However, the mean eccentricity index of all growth rings analyzed for the buried root samples was approximately 0.27 (Fig. 4c).

On average, the eccentricity index of the growth rings after exposure was, approximately, 0.48 and the eccentricity index of the growth rings before the erosive process was, approximately, 0.32, similar to the eccentricity index of the rings of the buried samples (Fig. 4c). Figure 5b shows a relatively low percentage of growth rings in the buried samples with an eccentricity index higher than 0.5 and 0.75.

For exposed roots, there was an increase in the eccentricity index in the most recent growth rings, that is, at the end of the growth ring series (Fig. 6). The exposed roots had a high eccentricity index at the end of the growth ring series (> 0.75), delimiting the concentric phase of the roots in the oldest growth rings (beginning of the series) and the eccentric phase of the roots (end of the series). In

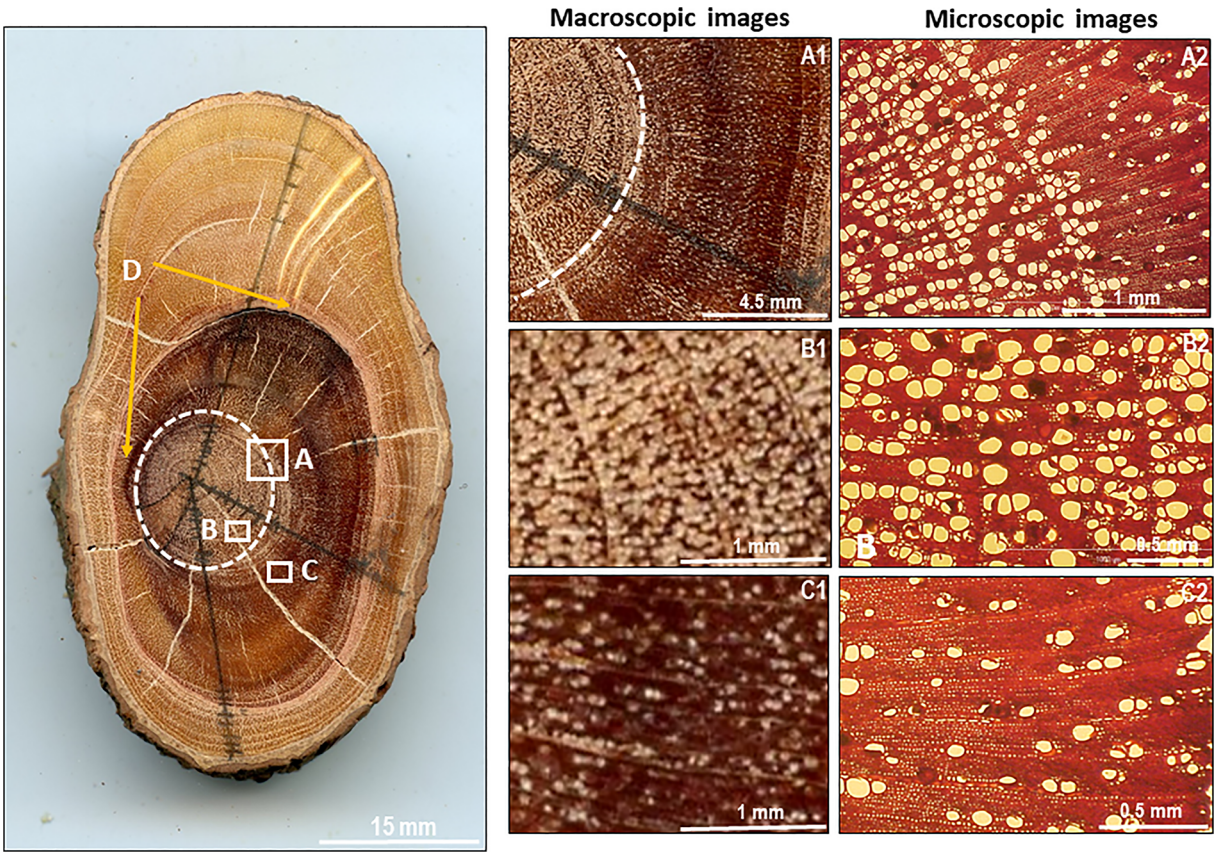

Fig. 2 Left image: sample of exposed root. **a** delimitation of concentric to eccentric growth; **b** vessel frequency before the appearance of eccentricity; **c** vessel frequency after the appearance of eccentricity; **d** scar in the first growth ring after exposure

Fig. 6b, a significant increase in the relative percentage of samples with an eccentricity greater than 0.5 and 0.75, after the approximate year of 1994 is noted.

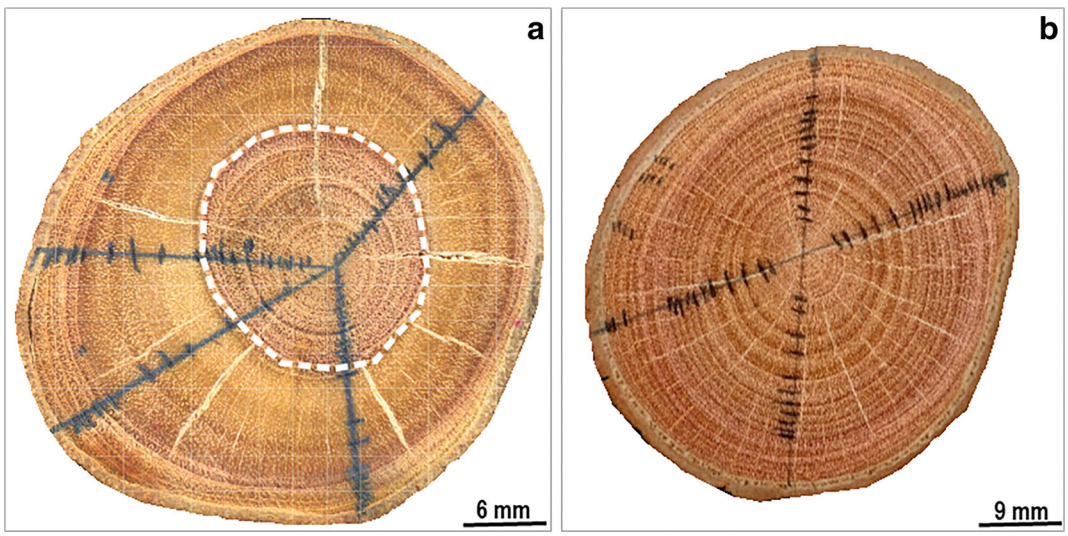

Fig. 3 Example of root samples. **a** exposed root: delimitation of the concentric phase and the eccentric phase; **b** buried: concentric growth rings

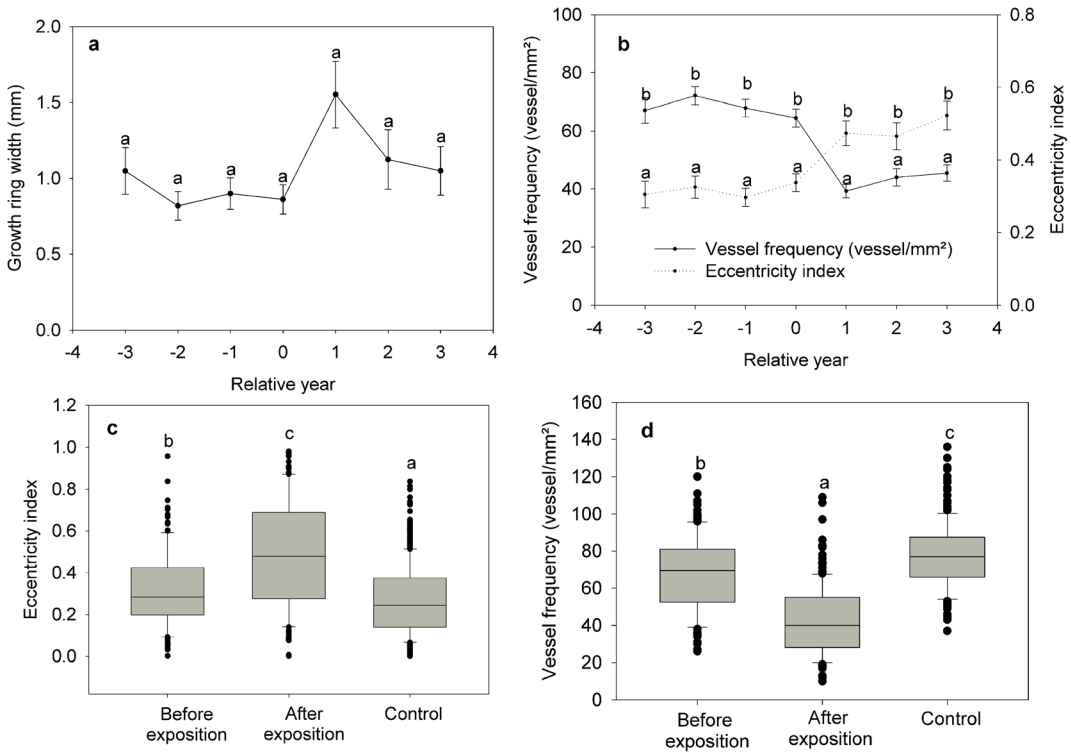

Fig. 4 Variations of the mean (and standard error) over the relative years of exposed and buried roots: **a** in growth ring width and **b** in vessel frequency and eccentricity index. Year zero represents the first year of exposure. Negative values represent unexposed rings, and positive values represent exposed rings. Quantification of the anatomical changes (eccentricity and frequency of vessels) associated with the rings before exposure, after exposure and rings of buried samples: **c** eccentricity index and **d** vessel frequency. Means followed by different letters indicate statistically significant differences ($p < 0.05$)

In addition to changes in the growth pattern from concentric to eccentric, anatomic reactions occurred in the growth rings after exposure. The first year of exposure can be determined precisely by the microscopic characterization of the anatomical changes that occur in the wood (Hitz et al. 2008). In this sense, the growth rings after exposure showed a decrease in the frequency of vessels. The Fig. 4b shows the decrease in vessel numbers concomitantly with the increase in eccentricity is documented. From year zero (exposure year) to year 1 (after exposure) a 39% drop in vessel number was observed. There are statistically significant differences in vessel frequency between the samples of growth rings before and after the erosive process. Likewise, there is a statistically significant difference between the growth rings before the exposition and the buried group.

Regarding the appearance of scars, 37% of exposed root samples showed scars and 18% of scars appeared concomitantly at the first/s year of exposure. The remaining of the scars appeared in later years; however, all appeared in years after the first year of exposure. Figure 7 shows the approximate position (angle) of the scar appearance, for all cross-sections of all exposed roots that showed scars. It is noted that 83.3% of the scars appears in the upper part of the root and only 16.6% of the scars appears in the quadrants of the lower part of the root (3 scars of 3 different exposed roots). However, some of them are directed towards the opposite side to erosive flow. The scars that appeared in the lower quadrants may have been formed when it was fully exposed.

Relation between root exposition, eccentricity and total precipitation

Figure 8a shows that the number of exposed roots per year begins to appear after 1983, an extremely rainy year. The exposition of the roots begins in the year 1988. The year 1982–1983 was marked by an El Niño event, responsible in the region of the

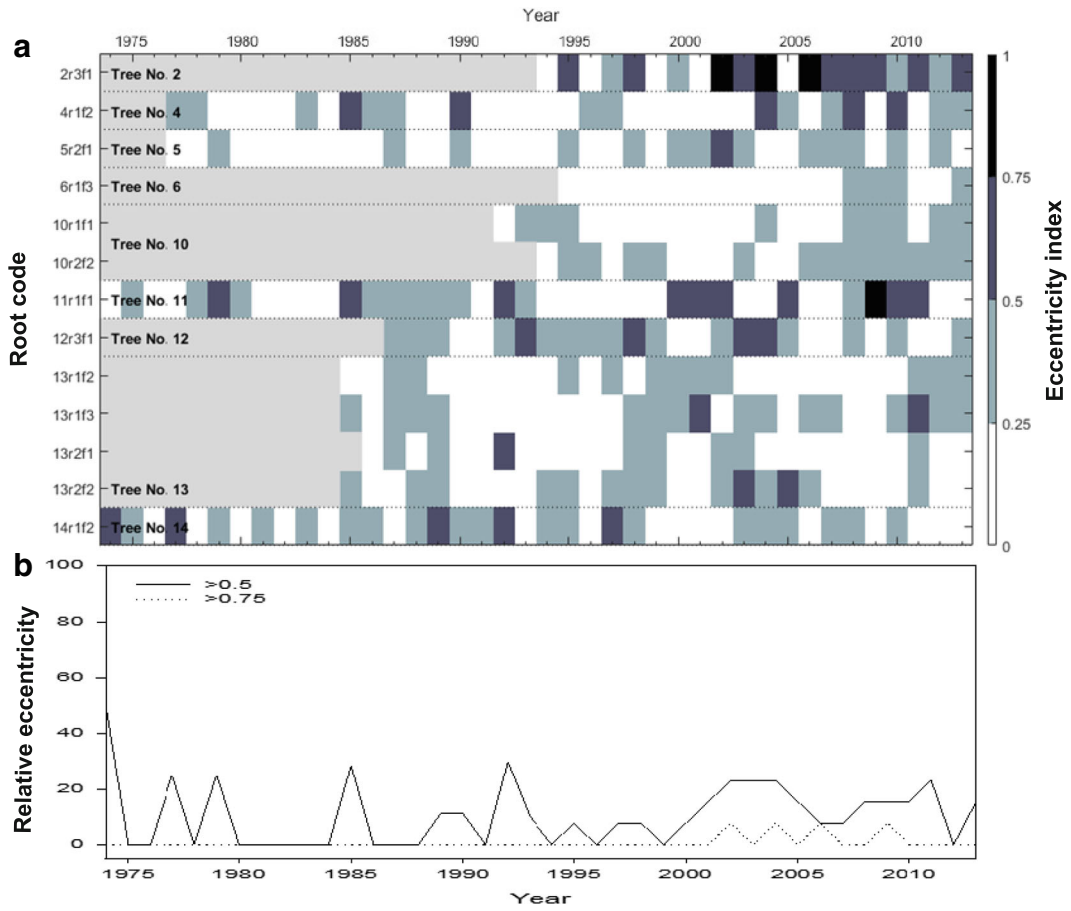

Fig. 5 Eccentricity index of the buried root samples: (**a**) eccentricity index values per analyzed sample and per year; (**b**) relative percentage of samples with an eccentricity index greater than 0.5 and 0.75. The samples are identified as follows: n, identification of the tree; r, identification of the buried root; fn, analyzed root slice. Example: 2r3f1: tree 2, exposed root 3, slice number 1

study area for more than 2,000 mm of rain (the long-term regional precipitation average is approximately 1,275 mm). The erosive event and the consequent exposure of the tree roots may have been initially triggered by this extreme rainfall. In the following years, the increase/decrease of the exposure of the roots together with the increase/decrease of the accumulated precipitation is verified. A high number of exposed roots in the years 1996 and 2000 is observed.

Figure 8b shows the number of exposed roots related to the relative proportion of samples with eccentricity >0.75. The eccentricity peaks/falls are related to the increase/decrease in the number of exposed roots, that is: the higher the number of exposed roots, the greater the total eccentricity index of the sample set. This index continues to increase until the end of the time series since the eccentricity tends to increase always after root exposure.

The Fig. 8c shows a relation between the accumulated precipitation and the relative percentage of samples, coincident with an eccentricity index greater than 0.75. Moreover, a relationship between the eccentricity peaks/falls with accumulated precipitation peaks/falls is slight.

Calculation of the erosion rate

We present in Table 1 the erosion rates allied to the type of erosive process for each exposed root. In Sector I, erosive processes were classified as piping, permanent gullies and ephemeral gullies, being responsible, on average, for the vertical soil loss of 0.81 cm year^{-1}, 1.07 cm year^{-1} and 1.70 cm year^{-1}, respectively. For

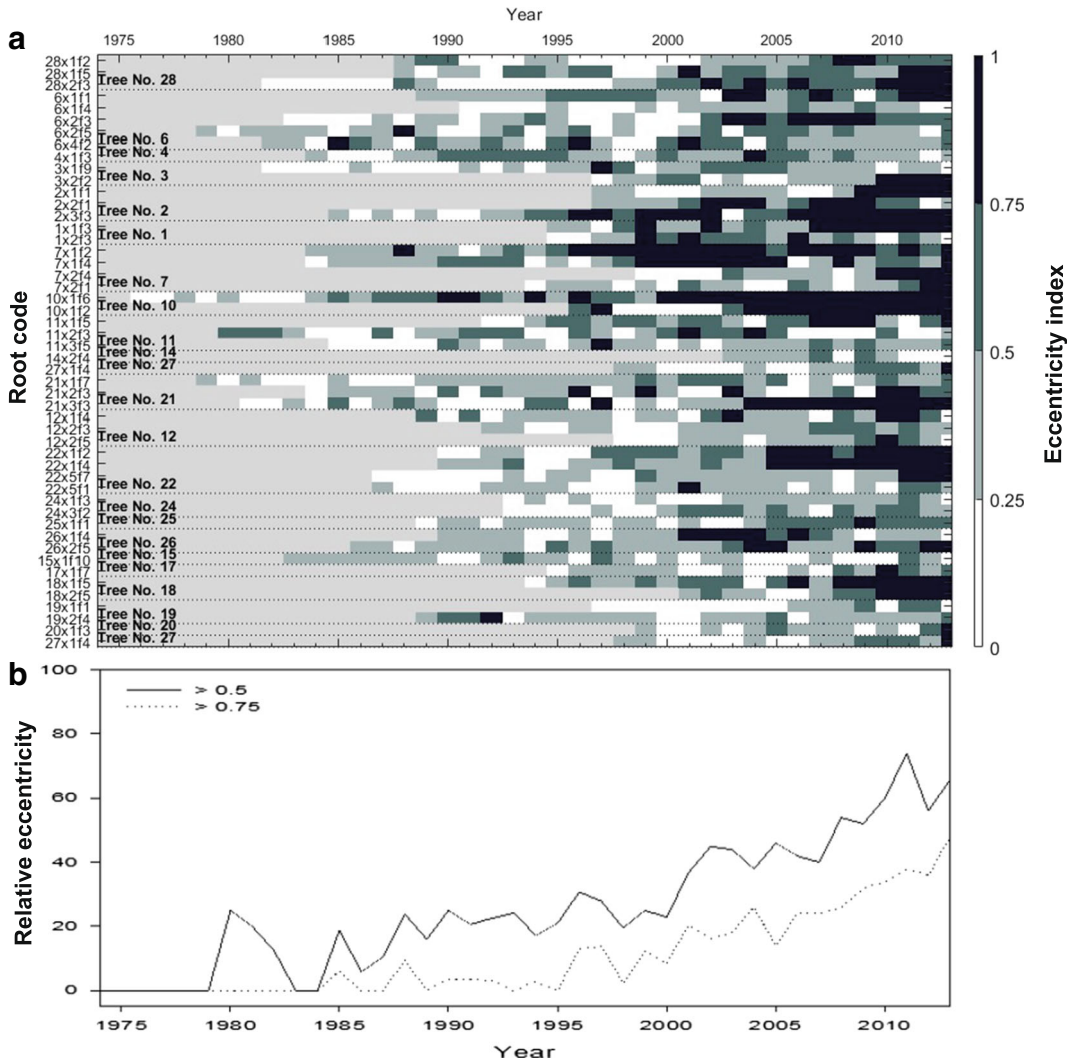

Fig. 6 Eccentricity index of the exposed root samples: (**a**) eccentricity index values per analyzed sample and per year; (**b**) relative percentage of samples with an eccentricity index greater than 0.5 and 0.75. The samples are identified as follows: n, identification of the tree; xn, identification of the exposed root; fn, analyzed root slice. Example: 2x3f1: tree 2, exposed root 3, slice number 1

Sector II, the average vertical soil loss was 0.58 cm year^{-1} for the piping erosion, 1.77 cm year^{-1} for permanent gully, 1.91 cm year^{-1} for ephemeral gully and 2.87 cm year^{-1} for sheet erosion. In Sector III, we only found gully and sheet erosion processes, with rate values of 0.73 cm year^{-1} and 4.10 cm year^{-1}, respectively.

The values found for the horizontal erosion rates were higher (Table 1). The expansion in length is more accelerated than the deepening of the soil by erosion. The values presented a high variability, and the gullies were responsible for the highest values, reaching in some cases more than 120 cm year^{-1}.

Discussion

Growth rings and tree ring indicators

The inter-correlations in the growth ring series of exposed and unexposed roots indicate high ring growth syncronization, which is a consequence of the influence of a dominant factor on growth, probably the climatic factor (Chartier et al. 2016). The mean sensitivity, with values above 0.30, shows that plants react to the environment through annual growth variability (Grissino-Mayer 2001).

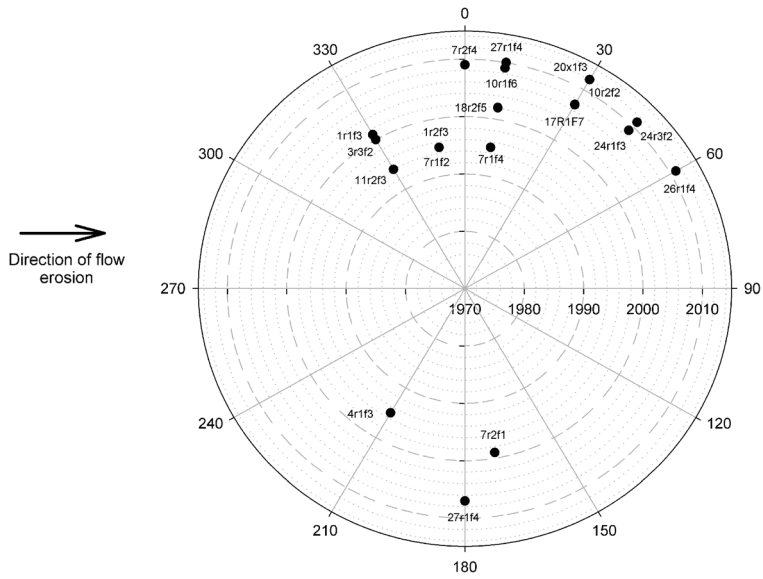

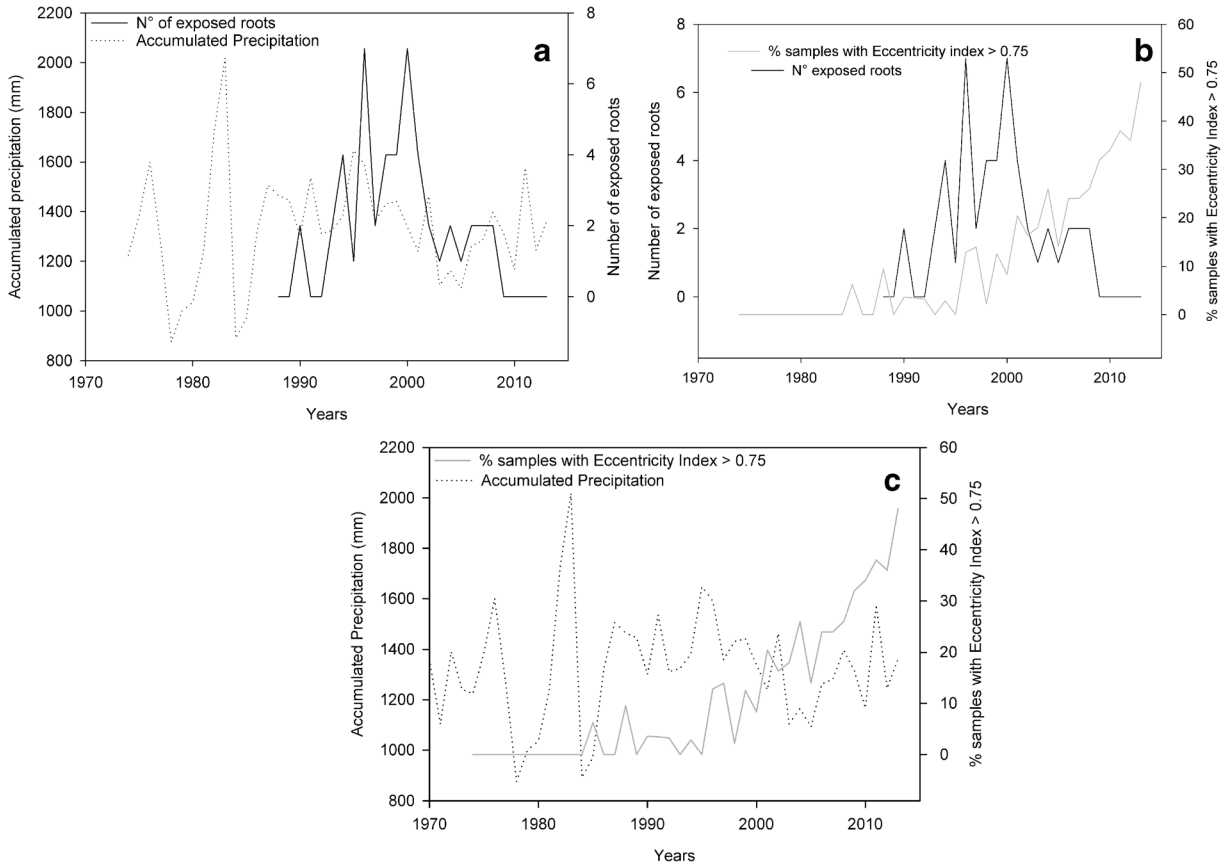

Fig. 7 Approximate location and scars dated of all exposed roots analyzed and the direction of erosion flow. Zero angle indicates the top of the root

Fig. 8 **a** Relation of the number of exposed roots and accumulated precipitation; **b** Relation of number of exposed roots and percentage of samples with eccentricity index greater than 0.75; **c** Relation of accumulated precipitation and percentage of samples with eccentricity index greater than 0.75

Table 1 Year of exposure, vertical erosion rate (VER) and horizontal erosion rate (HER) in cm year^{-1} for each type of erosion process and exposed root

		Year of root exposure	Height root-soil (cm)	Years after root exposure	VER	Horizontal distance (cm)	Year of exposure neighboring roots	HER	Soil erosion process
Sector I	28x1f2	1994	13	19	0,68	r1-r2: 64	5	12.80	P
	28x1f5	1994	30	19	1.58				
	28x2f3	1999	8	14	0.57				
	6x1f1	2000	1	13	0.08	r1-r4: 128	1	128.00	G
	6x1f4	1997	18	16	1.13				
	6x2f3	2001	11	12	0.92				
	6x2f5	1998	21	15	1.40				
	6x4f2	1999	2	14	0.14				
	4x1f3	1994	8	19	0.42	–	–	–	P
	3x1f9	1996	91	17	5.35	r1-r3: 46	4	11.50	EG
	3x3f2	2000	7	13	0.54				
	2x1f1	2000	5	13	0.38	r1-r2: 32; r1-r3: 8	1.00	32.00	EG
	2x2f1	2001	2	12	0.17		7.00	1.14	
	2x3f3	1993	14	20	0.70				
	1x1f3	1996	13	17	0.76	r1-r2: 27	1	27.00	EG
	1x2f3	1996	13	17	0.76				
	7x1f2	1990	8	23	0.35	r1-r2: 93	9	10.33	G
	7x1f4	1990	24	23	1.04				
	7x2f4	2008	22	5	4.40				
	7x2f1	1999	2	14	0.14				
	21x1f7	2004	32	9	3.56	r1-r2: 23; r2-r3: 62	1	23.00	EG
	21x2f3	2003	37	10	3.70		7	8.86	
	21x3f3	1996	18	17	1.06				
Sector II	10x1f6	1988	25	25	1.00	r1-r2: 15	14	1.07	P
	10x2f2	2002	6	11	0.55				
	11x1f5	1993	63	20	3.15	r1-r2: 72	1	72.00	G
	11x2f3	1994	20	19	1.05				
	11x3f5	1996	24	17	1.41				
	14x2f4	2006	27	7	3.86	–	–	–	S
	27x1f4	2005	15	8	1.88	–	–	–	S
	12x1f4	2001	12	12	1.00	r1-r2: 65	4	16.25	EG
	12x2f3	2001	9	12	0.75				
	12x2f5	1997	18	16	1.13				
	22x1f2	1996	7	17	0.41	r1-r5: 80	2	40.00	EG
	22x1f4	1996	15	17	0.88				
	22x5f7	1998	137	15	9.13				
	22x5f1	2000	1	13	0.08				
	24x1f3	1998	6	15	0.40	r1-r3: 30	1	30.00	P
	24x3f2	1999	5	14	0.36				
Sector III	25x1f1	2000	2	13	0.15	–	–	–	G
	26x1f4	2000	17	13	1.31	40.00	–	48.00	G
	15x1f10	2007	87	6	14.50	–	–	–	S
	17x1f7	2007	39	6	6.50	–	–	–	S

Table 1 (continued)

	Year of root exposure	Height root-soil (cm)	Years after root exposure	VER	Horizontal distance (cm)	Year of exposure neighboring roots	HER	Soil erosion process
18x1f5	1995	25	18	1.39	r1-r2: 20	7	2.86	S
18x2f5	2002	25	11	2.27				
19x1f1	2006	3	7	0.43	r1-r2: 20	2	10.00	S
19x2f4	2004	16	9	1.78				
20x1f3	2008	9	5	1.80	–	–	–	S

Soil erosive processes: P: piping; G: gully; EG: ephemeral gully; S: sheet; n: ientification of the tree, xn: identification of exposed root, fn: analyzed root slice. Example: 2x3f1: tree 2, exposed root 3, slice number 1

The eccentricity index, vessel frequency, and width of the growth rings allowed the determination of the first year of root exposure, allowing the soil erosion rate calculation. These changes in the wood anatomical structure following the soil erosion process occur due to the exposition of the root to atmospheric conditions (for example, variations in temperature, reduction of soil layer pressure, incidence of light) and mechanical stress due to the impact of debris carried by soil erosion (Bodoque et al. 2011). Growth eccentricity is one of the most common and visible characteristics of change after exposure (Ballesteros-Cánovas et al. 2013; Stoffel et al. 2013). The starting point for determining the first year of exposure in the present study was the eccentricity index. Root eccentricity begin to manifest even before root exposure since unexposed growth rings of exposed roots already exhibit higher eccentricity rates. Trees suffering the influence of erosive processes can respond to soil instability, leading to the formation of eccentric growth rings even before exposition. On the contrary, together with the eccentric growth rings, there is a decrease in the frequency of vessels in the growth rings after the occurrence of the root exposition. This pattern is not universal, Chartier et al. (2016) indicate an increase in frequency of vessels and decrease in vessel area. These differing responses may be related to the species considered and their reaction to environmental changes.

Other anomaly that we found was that the number of vessels in the growth rings of the buried samples was higher than the number of vessels in the unexposed rings of the exposed roots. This wood anatomical change can be explained by the fact that the count of the number of vessels carried out in the buried samples covered the newest and the oldest growth rings, i.e., practically the whole series of growth rings. On the contrary, for the exposed root only three rings previous and three rings after the exposure process were analyzed. So, we can argue that the change in the number of vessels is occurring before the root is exposed. Similar results were found by Gärtner (2007), where it was shown that anatomical changes due to continuous denudation of the soil occur 30 mm before the root is exposed. More recently, Corona et al. (2011) demonstrated that in the case of continuous ground retraction, roots do not react to exposure with anatomical responses at the time these are exposed, also demonstrating that anatomical changes occur when the soil is reduced to, approximately, 30 mm from the root.

Similarly, the scars found in transverse sections of the exposed roots served to assist in the determination and confirmation of root exposition and also in the dating of unique events. In some root samples, the scars appeared in the first or second year after root exposure but in other cases these were coincident with the first year of exposure. In the study carried by Chartier et al. (2016), the scars were always coincident with the first year of root exposure. In this context, scars are formed by abrasion of the cambium tissue and are anatomically detected and easily dated (Ballesteros-Canovas et al. 2013). Considering others causative effects, after root expossure, the upper part of the root is more susceptible to effect of climatic factors (e.g., UV radiation, tissue drying and freezing) and to impact from rocks, debris, tree branches, and injuries caused by animals, among others. These disturbances are recorded in the root wood as scars and can be used as a means of dating geomorphological processes since the buried roots did not present the formation of scars.

The width of the growth rings did not find significant differences between the years before and after the erosive event. However, there is a tendency to increase the width of the first growth ring after exposure (year 1) (Fig. 2). The next growth rings (year 2 and 3) showed a

tendency of decrease in width. Similar results were also found by Ballesteros-Canovas et al. (2013), Bodoque et al. (2011) and Gärtner et al. (2001).

Reconstruction of erosion dynamics using exposed roots

Through the determination of the first year of root exposure, it was possible to reconstruct the dynamics of the erosive process, reaching a better understanding about the evolution of the erosive features and landscape changes. Figure 9 represents the erosive features with the location of the trees and exposed roots studied. For each exposed root there is a root exposure year.

For Sector I, the oldest date of root exposure was from the year 1990, coming from the gt7 tree. The roots of gt7 tree were in a branch of the main gully, where it is possible to verify the process of expansion of the drainage head by means of the observed exposure dates. The root r1, located more downstream, was exposed in 1990, and r2f1, located more upstream of the gully branch, was exposed 9 years later regardless of the height of the root to the current surface of the soil. Also, root r2f4 presented date of exposure in 2008; however, this section was located at the edge of the gully and may have been exposed more recently by the widening of the edge of the gully. In this same sector, the gt1 tree presents the same exposure date for the two roots studied: 1996. For gt1, the erosion feature was characterized as an ephemeral gully that will probably connect to the branched sector of the gully, causing its expansion. This ephemeral gully may have been formed by the process of subsurface erosion, which will later connect to the central erosion, since it is not linearly connected to a branch of the gully and neither to the main gully.

In the same way, tree gt2 follows the same pattern: roots r1 and r2 show similar dates of exposure (2000 and 2001). This erosion feature is not connected to the branch of the main gully. Tree gt3 presents date of exposition of root r3 in the year 2000, similar to the roots of the gt2 tree. However, r1 of this same tree presents date of exposure in the year 1996, but this root

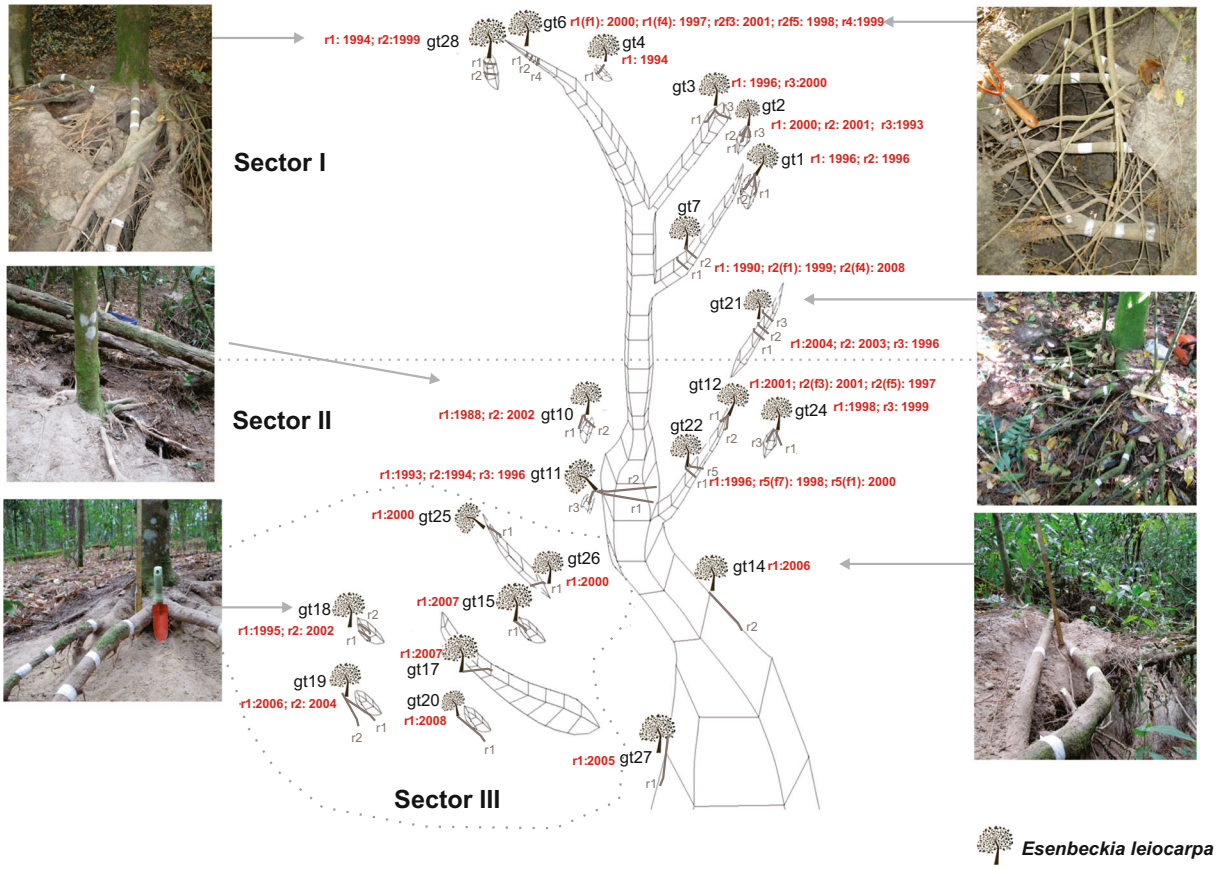

Fig. 9 Schematic representation of the erosive features and the location of trees and exposed roots along with exposure years

is much closer to the surface and close to the border of the wall of the erosive feature, demonstrating the process of deepening and lateral expansion of erosion. The gt4 tree presents an older period of root exposure (year 1994) corresponding to a piping erosive process. In general, in Sector I, the older exposures are related to the piping process, which may be related to the subsequent triggering of gully formation by subsurface erosion processes. The gt4 and gt28 trees, both influenced by the piping process, are in different locations, however, they present the same date of root exposure - the year 1994 -, indicating that this process can be co-occurring in different locations by the connection of subsurface ducts. These ducts connect linearly with each other and with the main gully (Díaz et al. 2007). The gt6 tree presents different exposure dates for the three roots studied. The roots closer to the drainage head, with the cross-section of the root located in the middle of the gully (r1f1 and r2f3), show the most recent dates of exposure (year 2000 and 2001), whilst the downstream root (r4) presents an earlier date of exposure (1999), indicating the process of backward movement of the drainage head. The roots r1f4 and r2f5, with exposure dates in 1997 and 1998, were located at the edge of the gully showing that the upslope expansion of the gully in this portion initiated from the borders inwards, probably was affected by the piping process.

For gt28 tree, the difference between the exposure of r1, located 8 cm from the soil surface, and r2, located at 30 cm, shows that the erosive process exposes first the roots closer to the current soil surface since r1 was exposed in 1994 and r2 in 1999. With r1 being closer to the soil surface and being exposed five years before r2, we can note a process of deepening and collapsing of the piping ceiling. On the other hand, gt21 tree presents a process of gully opening that starts upslope, where r3 is located, and evolves downslope in direction to r1. In general, for Sector I, the earliest date of the erosive process dates back to the year 1994. It should be remembered that this dating is restricted to the exposed roots that were found and collected in the field. Therefore, the erosive process may have started earlier. The relative percentage of samples with eccentricity index >0.75, verified in Fig. 6, increase in the period after 1994 suggesting that the erosion processes were more intense since then.

In Sector II, gt10 tree, which is influenced by piping, presents dates of root exposition in 1988 and 2002. The year 1988 is the oldest one found in this study. Possibly this cavity will connect to the central gully system since it is close to this system. For gt11 tree, r1 and r2 cross transversely the main gully. The date of exposure of these roots is 1993 and 1994, respectively for r1 and r2. Once again, the process of headcut retreat of the main gully was confirmed. The sampled roots of gt27 and gt14 trees are oriented parallel to the edge of the gully and showed very close exposure dates, namely 2005 and 2006, respectively. This information permits to chronologically evaluate the process of lateral expansion of the gully that occurred in more recent years of exposure. In this way, the dates obtained show the advancement of the gully in three directions: deepening, expansion of the lateral walls and headcut retreat (Toy et al. 2002). The gt24 tree, also influenced by piping, shows that the process occurs almost concomitantly with the opening of the gully, resulting in exposure dates close to the gt11 tree: 1998 and 1999 for roots 1 and 3, respectively. The trees gt22 and gt12 represent, once again, the process of headcut retreat of the gully branch, started in 1996 according to the gt22 tree evidence and with a new advance in the year 2001, according to the two analyzed roots of the gt12 tree.

Sector III is the one that presents the most recent dating and, for the most part, the sheet erosion was the dominant process. Although the root exposure dates are more recent, the process of sheet erosion in Sector III was the one that presented the highest soil losses when compared to the rest of the system. Only the gt25 and gt26 trees are being affected by gully erosion. Both trees are located in different positions along an ephemeral gully and the exposition year of the respective analyzed roots is the same (year 2000). This fact shows that the ephemeral gully was formed at the same time along its whole extension probably due to a partial collapsing of the ceiling of a pipe during that year. This partial collapsing of the pipe was not able to superficially connect the ephemeral gully to the main gully.

The system of gully opening influenced by piping

Soil erosion features disconnected from the main gully can be observed in the study area, in the form of ephemeral gullies. Three different types of ephemeral gullies can be found, according to their origin (Casalı et al. 1999): 1) classical ephemeral gully, formed by the concentration of surface flow that promotes localized degradation, which in turns causes the gully to migrate upstream, widening and deepening the gully channel; 2) drainage ephemeral gullies: formed by drainage flows that reach the upstream

end of a slope and form a gully in a downstream direction; 3) discontinuous ephemeral gully: usually found in places where there is an abrupt change in slope or areas of local instability. In this case, the headcut retreat can be triggered by the existence of areas of instability, such as small pipings (Casalı et al. 1999). In the study area, there are several dispersed areas of ephemeral gullies disconnected superficially from the main gully. Field observations, along with root exposure dating information, show that the formation of ephemeral gullies can originate in the process of headcut retreat of small pipings that appear on the surface after subsidence of the soil surface, as can be verified in the exposed roots of the gt1, gt2, gt4 and gt28 trees, for example.

Pipings are linearly connected in the subsurface and, in their expansion process, the tunnel ceiling loses its resistance, collapsing and causing the opening of a channel. There is a strong association between the piping process and the gully formation related to the process of headcut retreat and the deepening and lateral branching of the gully (Díaz et al. 2007; Faulkner 2013; Jones 2004; Verachtert et al. 2013).

In the central gully, a "step erosion" (Online Resource 2 - brown circle) was observed at the connection between Sectors I and II. This is a typical feature of an integration system between two types of processes of gully opening: connected and disconnected from the local hydrography (De Oliveira 1989). In the disconnected system, the advance of the gully occurs upstream, forming a cone of sediment deposition downstream. This system corresponds to Sector II of the study area. In the connected system, a channel is connected to the main drainage system that develops by headward expansion. The system connected to the local hydrography (Sector I of the study area) may have been caused by concentrated surface flow causing excavation and channel widening. The trigger of this process is a complex combination of concentrated surface flow and mass movement. The integration of the connected and disconnected systems, where the slope becomes flatter, is considered the final stage of gully evolution (De Oliveira 1989).

The study area presents a complex erosive system composed of several stages and types of erosion that currently evolve concomitantly. In summary, this system was divided into three sets of processes: 1) initial process - the oldest gully - consisting of the most advanced erosion process; represents the deepest part of the gully, reaching the parent material, responsible for great soil loss; 2) an intermediate process, encompassing the ephemeral gullies and the branches of the central gully, responsible for massive soil losses and influenced by the piping process for the formation and retraction of the drainage head which, over time, will connect with the central gully; 3) more recent erosion features in the form of sheet erosion (some already reaching the ephemeral gully stage) located in Sector III that represent the less evolved erosion processes of the study area, however, responsible for massive soil losses.

Estimative of the erosion rate using exposed roots

The lowest values of soil loss rate were recorded in piping and the highest values in the sheet erosion process (Table 1). However, subsurface erosion in pipes should be considered of extreme importance, since it is responsible for triggering of gullies with vertical walls (Díaz et al. 2007). The permanent gully, because it is a more evolved and possibly more stabilized process, presented smaller soil loss values when compared to ephemeral gullies. For the horizontal evolution of the erosion features, the values found were high. This type of process is represented by the headcut retreat of the gully, demonstrating its expansion horizontally. The upslope linear process occurs faster than the process of deepening.

Thigh erosion rates found in the study area mainly related to a combination of factors that involves intense and concentrated rainfalls, but also because it presents a soil highly susceptible to erosive processes and favorable to the formation of subsurface erosion, which triggers and accelerates surface linear erosion features. In tropical countries, rainfall is the main erosive agent responsible for soil degradation and loss, having a positive correlation between rainfall intensity and rainfall erosion rate (Chaplot and Le Bissonnais 2000; Iserloh et al. 2013). Online Resource 3 shows a relationship between total precipitation and the number of erosive rainfalls, where the highest number of erosive rainfalls is related to the increase in total precipitation of the year. Consequently, there is an increase (decrease) in the number of exposed roots and eccentricity index with increasing (decreasing) accumulated total precipitation (Fig. 8), and this, in turn, is directly related to the increase in the number of erosive rainfalls.

The Gärtner (2007) equation used to calculate soil loss was initially developed for sheet erosion rate calculations. However, in the present study, the equation used by Gärtner was also used for gullies, ephemeral gullies, and piping. This approach has brought a significant

understanding of the deepening process of gullies and pipings. In contrast, the Malik equation was used for all types of erosive processes with the presence of exposed neighboring roots.

Conclusions

In this paper we present the use of a tropical tree species in the application of an existing dendrogeomorphological method—the analysis of wood anatomical structure in exposed roots—for determining the first year of exposure. This contribution presents novel information on the application of dendrogeomorphology in the tropics.

We demonstrated that anatomical changes in growth rings of exposed roots, such as increase in vessel frequency, increase in ring eccentricity and increase in growth ring width can be used to determine the first year of root exposure. In addition, the formation of scars was also used in the dating of exposed growth rings by soil erosion. Consequently, this analysis allowed to quantify and evaluate the erosive process dynamics of complex systems in Hapludult soils, in time and space, helping to infer soil erosion rates vertically and horizontally. We verify the impact of piping on gully initiation and development. The subsidence of the soil surface by piping is responsible for the formation and evolution of the ephemeral gullies and the branching of the central gully. The heavy rains proved to be linked to the beginning of the erosive processes, as evidenced by the dendrochronological dates obtained through the exposed roots.

Erosive and geomorphological processes are complex, and the reconstruction of their dynamics and history is always a challenge. The presence of trees with exposed roots or buried stems can act as a real living testimony to these processes of geomorphological evolution, either downhill or surface uplift, on a temporal and spatial scale Therefore, dendrogeomorphology is a powerful tool for the reconstruction of past events and for the calculation of the speed of this process.

Acknowledgments The authors thank the National Council for Scientific and Technological Development (CNPq) for a graduate scholarship, fellowship and financing of the project. They also thank Jonathan Barichivich for the help in preparing the software scripts used in this paper and the reviewers for the valuable suggestions and comments that permitted to improve the manuscript.

References

Alvares CA, Stape JL, Sentelhas PC, Gonçalves JLM (2013b) Modeling monthly mean air temperature for Brazil. Theor Appl Climatol 113(3–4):407–427. https://doi.org/10.1007/s00704-012-0796-6

Alvares CA, Stape JL, Sentelhas PC, Gonçalves JLM, Spavorek G (2013a) Köppen's climate classification map for Brazil. Meteorol Z 22(6):711–728. https://doi.org/10.1127/0941-2948/2013/0507

Ballesteros-Cánovas JA, Bodoque JM, Lucía A, Martín-Duque JF, Díez-Herrero A, Ruiz-Villanueva V, Rubiales JM, Genova M (2013) Dendrogeomorphology in badlands: methods, case studies and prospects. Catena 106:113–122. https://doi.org/10.1016/j.catena.2012.08.009

Bodoque JM, Lucía A, Ballesteros JA, Martín-Duque JF, Rubiales JM, Genova M (2011) Measuring medium-term sheet erosion in gullies from trees: a case study using dendrogeomorphological analysis of exposed pine roots in Central Iberia. Geomorphology 134:417–425. https://doi.org/10.1016/j.geomorph.2011.07.016

Bodoque JM, Ballesteros-Cánovas JA, Lucía A, Díez-Herrero A, Martín-Duque JF (2015) Source of error and uncertainty in sheet erosion rates estimated from dendrogeomorphology. Earth Surf Process 40:1146–1157. https://doi.org/10.1002/esp.3701

Braam RR, Weiss EEJ, Burrough PA (1987) Spatial and temporal analysis of mass movement using dendrochronology. Catena 14:573–584

Casalı J, López JJ, Giráldez JV (1999) Ephemeral gully erosion in southern Navarra (Spain). Catena 36:65–84. https://doi.org/10.1016/S0341-8162(99)00013-2

Chaplot V, Le Bissonnais Y (2000) Field measurements of interrill erosion under\- different slopes and plot sizes. Earth surf process Landf 25:145-153. https://doi.org/10.1002/(SICI)1096-9837(200002)25:2<145::AID-ESP51>3.0.CO;2-3 cited by: 77

Chartier MP, Giantomasi MA, Renison D, Roig FA (2016) Exposed roots as indicators of geomorphic processes: a case-study from Polylepis mountain woodlands of Central Argentina. Dendrochronologia 37:57–63. https://doi.org/10.1016/j.dendro.2015.11.003

Corona C, Saez JL, Rovéra G, Stoffel M, Astrade L, Berger F (2011) High resolution, quantitative reconstruction of erosion rates based on anatomical changes in exposed roots at Draix, Alpes de haute-Provence—critical review of existing approaches and independent quality control of results. Geomorphology 125:433–444. https://doi.org/10.1016/j.geomorph.2010.10.030

De Oliveira MAT (1989) Erosion disconformities and gully morphology: a threedimensional approach. Catena 16:413–423. https://doi.org/10.1016/0341-8162(89)90024-6

Díaz AR, Sanleandro PM, Soriano AS, Serrato FB, Faulkner H (2007) The causes of piping in a set of abandoned agricultural terraces in Southeast Spain. Catena 69:282–293. https://doi.org/10.1016/j.catena.2006.07.008

Faulkner H (2013) Badlands in marl lithologies: a field guide to soil dispersion, subsurface erosion and piping-origin gullies.

Catena 106:42–53. https://doi.org/10.1016/j.catena.2012.04.005

Gärtner H (2007) Tree roots—methodological review and new development in dating and quantifying erosive processes. Geomorphology 86:243–251. https://doi.org/10.1016/j.geomorph.2006.09.001

Gärtner H, Schweingruber FH, Dikau R (2001) Determination of erosion rates by analyzing structural changes in the growth pattern of exposed roots. Dendrochronologia 19:81–91

Grissino-Mayer HD (2001) Evaluating crossdating accuracy: a manual and tutorial for the computer program COFECHA. Tree-Ring Res 57:205–221

Hitz OM, Gärtner H, Heinrich I, Monbaron M (2008) Application of ash (Fraxinus excelsior L.) roots to determine erosion rates in mountain torrents. Catena 72:248–258. https://doi.org/10.1016/j.catena.2007.05.008

Holmes RL (1983) Computer-assisted quality control in tree-ring dating and measurement. Tree-Ring Bull 43:69–78

Howell BE, Mathiasen RL (2004) Growth impacts of Psittacanthus angustifolius Kuijt on Pinus oocarpa Schiede in Honduras. For Ecol Manag 198:75–88. https://doi.org/10.1016/j.foreco.2004.03.047

Hudson NW (1965) The influence of rainfall on the mechanics of soil erosion: with particular reference to southern Rhodesia. University of Cape Town, Cape Town

IAWA Committee (1989) IAWA list of microscopic features for hardwood identification. IAWA Bull 10:219–332

IBGE (2007) Manual Técnico de Pedologia. Fundação Instituto Brasileiro de Geografia e Estatística, Rio de Janeiro

Iserloh T, Ries JB, Cerdà A, Echeverría MT, Fister W, Geißler C, Kuhn NJ, León FJ, Peters P, Schindewolf M, Schmidt J, Scholten T, Seeger M (2013) Comparative measurements with seven rainfall simulators on uniform bare fallow land. Z Für Geomorphol Suppl Issues 57:11–26. https://doi.org/10.1127/0372-8854/2012/S-00085

Jones JAA (2004) Implications of natural soil piping for basin management in upland Britain. Land Degrad Dev 15:325–349. https://doi.org/10.1002/ldr.618

Lal R (2001) Soil degradation by erosion. Land Degrad Dev 12:519–539. https://doi.org/10.1002/ldr.472

Lawler DM (2005) The importance of high-resolution monitoring in erosion and deposition dynamics studies: examples from estuarine and fluvial systems. Geomorphology 64:1–23. https://doi.org/10.1016/j.geomorph.2004.04.005

Lisi CS, Tomazello-Filho M, Botosso PC, Roig FA, Maria VR, Ferreira-Fedele L, Voigt AR (2008) Tree-ring formation, radial increment periodicity, and phenology of tree species from a seasonal semi-deciduous forest in Southeast Brazil. IAWA J 29:189–207. https://doi.org/10.1163/22941932-90000179

Pimentel D, Harvey C, Resosudarmo P, Sinclair K, Kurz D, McNair M, Crist S, Shpritz L, Fitton L, Saffouri R, Blair R (1995) Environmental and economic costs of soil erosion and conservation benefits. Science 267:1117–1122

Poesen J (2018) Soil erosion in the Anthropocene: research needs. Earth Surf Proces Landf 43:64–84. https://doi.org/10.1002/esp.4250

Poesen J, Nachtergaele J, Verstraeten G, Valentin C (2003) Gully erosion and environmental change: importance and research needs. Catena 50:91–133. https://doi.org/10.1016/S0341-8162(02)00143-1

Santos HG, Carvalho Junior WD, Dart RDO, Áglio MLD, de Sousa JS, Pares JG, Fontana A, Martins AL da S, Oliveira AP (2011). O novo mapa de solos do Brasil: legenda atualizada. Embrapa Solos-Documentos, Rio de Janeiro

Šilhán K, Stoffel M (2015) Impacts of age-dependent tree sensitivity and dating approaches on dendrogeomorphic time series of landslides. Geomorphology 236:34–43. https://doi.org/10.1016/j.geomorph.2015.02.003

Stoffel M, Corona C, Ballesteros-Cánovas JA, Bodoque JM (2013) Dating and quantification of erosion processes based on exposed roots. Earth-Sci Rev 123:18–34. https://doi.org/10.1016/j.earscirev.2013.04.002

Toy TJ, Foster GR, Renard KG (2002) Soil erosion: processes, predicition, measurement, and control. John Wiley & Sons, New York

Trimble SW, Crosson P (2000) US soil erosion rates–myth and reality. Science 289:248–250. https://doi.org/10.1126/science.289.5477.248

Verachtert E, Van Den Eeckhaut M, Poesen J, Deckers J (2013) Spatial interaction between collapsed pipes and landslides in hilly regions with loess-derived soils: poorly drained landslides may create favourable conditions for piping. Earth Surf Process Landf 38:826–835. https://doi.org/10.1002/esp.3325

Vidal-Torrado P, Lepsch IF (1999) Relações material de origem / solo e pedogênese em uma seqüência de solos predominantemente argilosos e Latossólicos sobre psamitos na Depressão Periférica Paulista. Rev Bras de Ciência do Solo 23:357–369

Woodward DE (1999) Method to predict cropland ephemeral gully erosion. Catena 37:393–399. https://doi.org/10.1016/S0341-8162(99)00028-4